Carbohydrate Polymers 106 (2014) 469–474

Contents lists available at ScienceDirect

Carbohydrate Polymers

journal homepage: www.elsevier.com/locate/carbpol

Completely green synthesis of dextrose reduced silver nanoparticles, its antimicrobial and sensing properties

Sneha Mohan[a], Oluwatobi. S. Oluwafemi[b,*], Soney. C. George[c], V.P. Jayachandran[d], Francis B. Lewu[e], Sandile P. Songca[f], Nandakumar Kalarikkal[a,g], Sabu Thomas[a,h]

[a] Centre for Nanoscience and Nanotechnology, Mahatma Gandhi University, Kottayam, Kerala 686560, India
[b] Department of Chemistry, Cape-peninsula University of Technology, P.O.Box 652, Cape town, 8000, South Africa
[c] Amal Jyothi College of Engineering, Kanjirappally, Kottayam, Kerala 686560, India
[d] Antibacterials and Microbial Technology Lab, Pushpagiri Research Centre, Pushpagiri Institute of Medical Sciences, Tiruvalla, Kerala 689 101, India
[e] Department of Agriculture, Cape-peninsula University of Technology, Wellington, 7655, South Africa
[f] Department of Chemistry, Walter Sisulu University, Private Bag X1, Mthatha, 5117, Eastern Cape, South Africa
[g] School of Pure and Applied Physics, Mahatma Gandhi University, Kottayam, Kerala 686560, India
[h] School of Chemical Sciences, Mahatma Gandhi University, Kottayam, Kerala 686560, India

ARTICLE INFO

Article history:
Received 8 October 2013
Received in revised form
14 December 2013
Accepted 5 January 2014
Available online 13 January 2014

Keywords:
Green synthesis
Silver nanoparticles
Gelatin
Dextrose
Antibacterial
Sensor

ABSTRACT

We herein report the green synthesis of highly monodispersed, water soluble, stable and smaller sized dextrose reduced gelatin capped-silver nanoparticles (Ag-NPs) via an eco-friendly, completely green method. The synthesis involves the use of silver nitrate, gelatin, dextrose and water as the silver precursor, stabilizing agent, reducing agent and solvent respectively. By varying the reaction time, the temporal evolution of the growth, optical, antimicrobial and sensing properties of the as-synthesised Ag-NPs were investigated. The nanoparticles were characterized using UV–vis absorption spectroscopy, Fourier transform infra-red spectroscopy (FT-IR), X-ray diffraction (XRD), transmission electron microscopy (TEM) and high resolution transmission electron microscopy (HR-TEM). The absorption maxima of the as-synthesized materials at different reaction time showed characteristic silver surface plasmon resonance (SPR) peak. The as-synthesised Ag-NPs show better antibacterial efficacy than the antibiotics; ciproflaxin and imipenem against *Pseudomonas aeruginosa* with minimum inhibition concentration (MIC) of 6 μg/mL, and better efficacy than imipenem against *Escherichia coli* with MIC of 10 μg/mL. The minimum bactericidal concentration (MBC) of the as-synthesised Ag-NPs is 12.5 μg/mL. The sensitivity of the dextrose reduced gelatin-capped Ag-NPs towards hydrogen peroxide indicated that the sensor has a very good sensitivity and a linear response over wide concentration range of 10^{-1}–10^{-6} M H_2O_2.

1. Introduction

Noble metals in quantum size regime have generated a lot of interest among researchers from various disciplines over the last decades (Hermanson, Lumsdon, Williams, Kaler & Velev, 2001; Jennifer, Bettye, Maddux & James, 2007; Kim, Eunye, Kim, Park, & Park, 2007; Zhenhua et al., 2003). This is due to the unique and attractive, optical and electronic properties of metal nanoparticles (NPs) such as silver (Ag), gold (Au), platinum (Pt) etc., which are significantly different from those of bulk materials. These properties are being influenced by several parameters, most importantly their size and shape. Among these materials, interest in Ag-NPs is very high due to their outstanding plasmonic activity, bacterial inhibitory and bactericidal effects compared with the other metal nanoparticles. The design of Ag-NPs especially using the bottom-up technique has been widely investigated for various applications and researchers are continuously developing newer methods for the synthesis of highly monodispersed and stable nanoparticles. Conventionally, stable metal nanomaterials are synthesized using either chemical or physical methods. In chemical methods, reducing agents like borohydrides, hydroxylamine hydrochloride, trisodium citrates, dimethylformamide etc are usually used (Chreigton, Blatchford & Albrecht, 1979; Lee & Meisel, 1982). The two main problems normally associated with the chemical synthetic route are the aggregation of the nanoparticles formed and the toxicity of the reagents used. As part of developing eco-friendly method, in order to address these concerns, new synthetic

* Corresponding author. Tel.: +27 765110322.
E-mail addresses: oluwafemi.oluwatobi@gmail.com (Oluwatobi.S. Oluwafemi), sabupolymer@yahoo.com (S. Thomas).

0144-8617/$ – see front matter © 2014 Elsevier Ltd. All rights reserved.
http://dx.doi.org/10.1016/j.carbpol.2014.01.008

routes based on green chemistry principles are being developed (Bozanic, Trandafilovic, Luyt, & Djokovic, 2010; Raveendran, Fu & Wallen, 2006).

There has been an upsurge of interest in implementing green chemistry principles into the synthesis of silver nanoparticles in order to maximize safety and efficiency, and minimise the environmental and societal impact of these materials. In the green synthesis of silver nanoparticles, three important factors to be considered are: (i) use of green solvents, (ii) use of an eco-friendly benign reducing agent, and (iii) use of a nontoxic material as a stabilizer. One of the green methods for preparing silver nanoparticles is the polysaccharide method. In this method, water is normally used as an eco-friendly benign solvent and polysaccharides as capping agents. Raveendran et al. (2003) reported the first completely green synthesis of Ag nanoparticles using water, starch and β-D-glucose as the solvent, capping agent and reducing agent respectively (Raveendran, Fu & Wallens, 2003). The use of starch makes it possible to avoid the use of relatively toxic organic solvents. Based on the modification of this method, synthesis of Ag-NPs have been reported using different sugars as reducing agent (Panacek et al., 2006) and biopolymers such as starch (Batabyal, Basu, Das & Sanyal, 2007) gelatin (Darroudi, Ahmad, Abdullah & Ibrahim,2011), polyvinylpyrolindone (PVP) (Filippo, Serra & Manno, 2009)and so on as passivating agent with or without accelerating agent such as NaOH (Darroudi et al., 2011a,b; Filippo, Serra, Buccolieri & Manno,2010; Stevanovic, Kovacevic, Petkovic, Filipic & Uskokovic, 2011). In a new development, our group also reported the synthesis of small highly stable and monodispersed Ag-NPs using maltose, a disaccharides sugar as reducing agent while gelatin and starch were used as passivating agent without the use of any accelerating agent (Oluwafemi et al., 2013a; Oluwafemi et al., 2013b). In another development, Eid and Azzay reported the synthesis of anisotropic Ag-NPs using dextrose, trisodium citrate and NaOH as reducing agent, capping agent and accelerating agent respectively (Eid & Assay, 2012). In their report, different sizes of robust hollow flower like nanostructures were produced by changing the concentration of the $AgNO_3$, dextrose, NaOH and trisodium citrate. However, such capping and accelerating agent may be associated with environmental toxicity or biological hazards. In this work, we reported, the synthesis of highly monodispersed, water soluble, stable and smaller sized gelatin capped-silver nanoparticles (Ag-NPs) via a completely green method by using dextrose as reducing agent without any accelerating agent. The antibacterial property of the as-synthesised dextrose reduced, gelatin-capped Ag-NPs at different stages of growth were tested for the first time against *Escherichia coli* and *Pseudomonas aeruginosa*, which are multidrug resistant bacteria and were compared with two antibacterial drugs; imipenem and ciprofloxacin using disc diffusion method. In addition, the minimum inhibitory concentration (MIC) and minimum bactericidal concentration (MBC) of the as-synthesised Ag-NPs were also evaluated. Furthermore, the sensing property of the Ag-NPs against H_2O_2, one of the reactive oxygen species (ROS) that possess a serious threat to biological system was also investigated.

2. Experimental procedure

2.1. Materials

All the chemicals were of analytical grade and used as purchased without any further purification. $AgNO_3$ was purchased from Alba scheme, while gelatin, dextrose and H_2O_2 were from Merck. All glasswares used in the experiment were cleaned and washed thoroughly with double distilled water and dried before use. A cultivating medium, Mueller–Hinton broth, used in the antibacterial assays was supplied by HIMEDIA Chennai. *E. Coli* ATCC 10536, and *P. aregumosa* bacterial strains isolated from human clinical material were used.

2.2. Synthesis of dextrose reduced gelatin coated Ag-NPs

In a typical synthesis, 1.0 g of gelatin was added to 95 mL of distilled water in a round bottom flask and heated to 40 °C to get a clear solution. 5 mL of $AgNO_3$ solution (1 M) was added to the gelatine solution with continuous stirring to obtain Ag^+/gelatin solution. This was followed by the addition of 10 mL dextrose solution (0.07 M) under continuous stirring. The reaction was maintained at 70 °C and allowed to react for several hours. Aliquots were taken at different time intervals to monitor the growth of the particles.

2.3. Characterization

A SHIMDTH UV 2401PC spectrophotometer was used for the absorption measurement in the 300–700 nm wavelength range. FT-IR spectra were recorded with Nicolet-Nexus 670. A JEOL JEM-3010 electron microscope operating at 200 kV was used for the TEM and HRTEM measurements. XRD measurements were performed on the Bruker D8 Advance diffractometer operating in the reflection mode with Cu-Kα radiation (40 kV, 20 mA) and diffracted beam monochromator. The samples for the XRD measurements were prepared by casting the silver nanoparticle solution on glass substrate and subsequently air-drying under ambient conditions.

2.4. Antimicrobial and bactericidal assays

2.4.1. Evaluation of antibacterial activity of nanoparticles

Antibacterial activity was evaluated using disc diffusion method. Mueller–Hinton broth (MHB) cultures (18 h) of two clinical isolates of *E. coli* and *P. aeruginosa* were evaluated in this study. 10 mg of the compound was dissolved in 1 mL sterile MilliQ water. 10 μL of the Ag-NPs solution was added on filter paper disc and dried at 30 °C in an incubator. A stock solution of $AgNO_3$ was made with the same concentration and checked for the purpose of comparison. Strict aseptic conditions were maintained throughout the procedure. Bacterial cultures were swabbed on Mueller–Hinton agar (MHA) plate and surface of the media was allowed to dry for 30 min, then the nanoparticles incorporated discs were pressed gently on the agar surface at specified distance. Ciprofloxacin (5 μg) and imipenem (10 μg) discs were also pressed separately on the agar surface for the purpose of comparison. After incubation at 37 °C for overnight, formation of inhibition zone was checked and diameter of zone was measured.

2.4.2. Determination of minimum inhibitory concentration (MIC) and minimum bactericidal concentration (MBC)

MHB broth culture (18 h) of clinical isolates of *E. coli* and *P. aeruginosa* isolates was selected for the evaluation of MIC. The assay was performed in 96-well microtitre plates. Inoculum density of the test organisms was adjusted to that of 0.5 Mc Farland standards (10 μL, $1 \times 10^{8-}$ CFU/mL). Broth was dispensed into the wells of microtitre plate followed by addition of the Ag-NPs solution and inoculum. Serial dilutions were performed by addition of various quantities of Ag-NPs solution to the microtitre wells with MHB to reach concentrations of 10– 100 μg/mL. The antibiotic imipenem and ciprofloxacin was also serially diluted with broth at a concentration ranging from 8–128 μg/mL. Microtitre wells containing fresh medium served as a negative control and that containing bacterial growth served as a positive control. Total volume of the assay system in each well was kept at 200 μL. Plates were incubated at 37 °C for 18 h and read at 600 nm in a plate reader (BIORAD 680). MIC was recorded as the lowest concentration at which growth was

observed. The measurements were done in triplicate. The content of the wells showing no visible growth as well as the positive and negative controls were subcultured on nutrient agar plates by streaking and incubated at 37 °C for overnight. On incubation of the plates, the dilution from the minimum concentration from those streaks showing no growth was considered as MBC. The highest dilution showing at least 99% inhibition is taken as MBC.

2.5. Study of H_2O_2 sensing by gelatin coated silver nanoparticles

The sensing property of the as-synthesized silver NPs was evaluated following the Endo, Yanagida, & Hatsuzawa, 2008 method (Endo et al., 2008) with slight modification. Different concentrations of hydrogen peroxide solutions (1000 μL) were introduced into the silver nanoparticle solution in a quartz cuvette at a ratio of 1:1.5. The change in the UV–vis spectrum with varying concentrations of H_2O_2 due to the catalytic reaction between silver nanoparticles and hydrogen peroxide was monitored.

3. Results and discussions

3.1. Characterisation of the as-synthesised Ag-NPs

In this reaction, the colour of the Ag^+/gelatin solutions in the reaction flasks changes from colourless to light brown and then dark brown as the reaction time increases, indicating the formation of dextrose reduced gelatin-capped Ag-NPs of different particle sizes. Dextrose can reduce silver cations to metallic silver and become oxidized to gluconic acid. The gradual formation and growth of silver nanoparticles at different reaction times were studied using UV–vis spectroscopy. The UV–vis spectra of the as-prepared samples at different reaction times are shown in Fig. 1. The obtained Ag-NPs displayed absorption maxima peaks characteristic of surface plasmon resonance (SPR) band for silver. The shift in the SPR peak can be related to the formation of silver nanoparticles

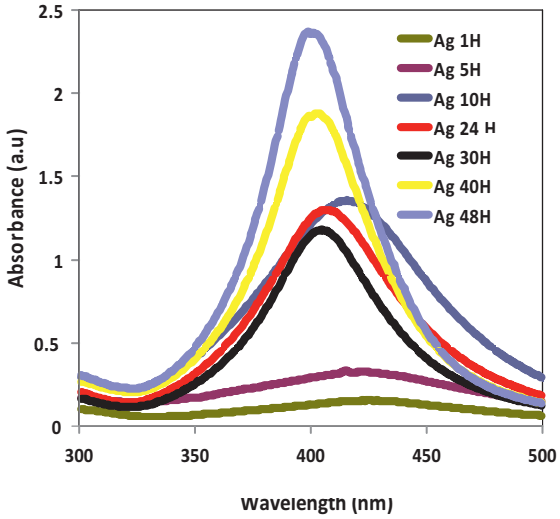

Fig. 1. Absorption spectra of dextrose reduced gelatin capped-Ag-NPs at different reaction time.

of different particle sizes. The characteristic absorption maximum peak of the as-synthesised Ag-NPs was gradually blue-shifted from 424 nm to 400 nm with increase in intensity as the reaction time increased. This indicates that as the reaction time increased, the particle size of the silver nanoparticles decreased. The increase in the intensity of the SPR peak as the reaction time increased indicates continued reduction of silver ions and increase in the concentration of the Ag-NPs. The sudden drop in the absorbance profile at 24 and 30 h is due to the dilution of the solutions at these reaction times and above. The broadness of the SPR peak also decreased with reaction time indicating particles with narrow size distribution.

The typical TEM morphologies of the as-prepared Ag-NPs at different reaction times of 1 h, 24 h and 48 h are shown in Fig. 2A–C.

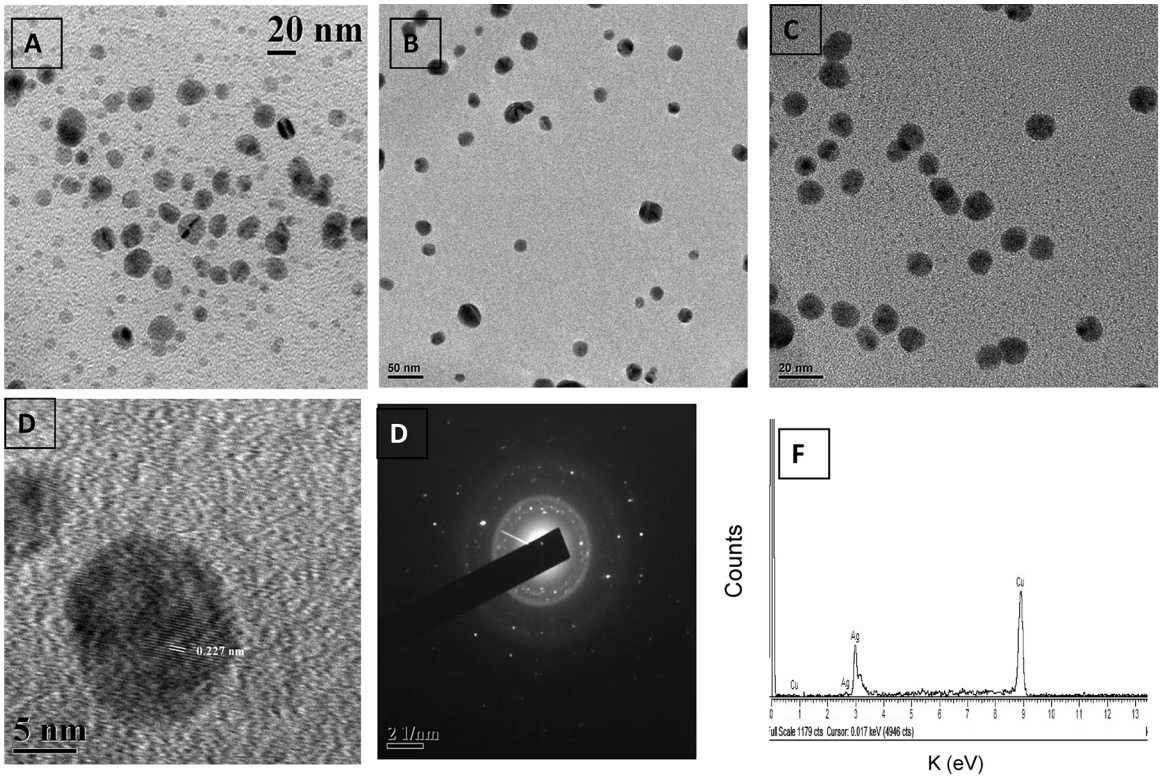

Fig. 2. TEM Images at 1 h (A), 24 h (B), 48 h (C), typical HRTEM image (D), SAED (E) and EDS (F) of dextrose reduced Ag-NPs.

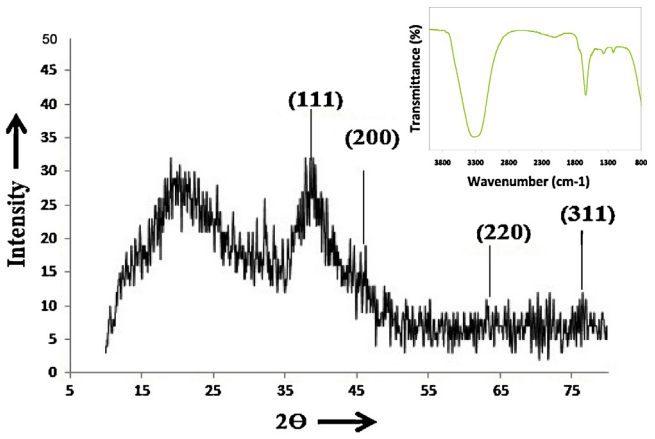

Fig. 3. Typical XRD pattern of the as-synthesised silver nanoparticles at 48 h and FT-IR spectrum (inlet).

The TEM results indicate that the particles are well dispersed and spherical in shape. The average particle diameter, as determined from the TEM images are 18.01 ± 5.54 nm (1 h), 9.98 ± 4.61 nm (24 h) and 9.68 ± 1.44 (48 h). The decrease in the average particle diameter and size distribution (σ), as the reaction time increases, is in agreement with the absorption spectra. The results also indicate that samples obtained over a long period of time retained a narrower particle size distribution with high level of uniformity. Similar observation has been reported by Darroudi et al. (Darroudi et al., 2011a,b). The HRTEM images (Fig. 2D) give further insight into the microstructure (shape) and crystallinity of the as-prepared Ag-NPs. The HRTEM image shows that the as-synthesised materials are spherical and consist of well ordered single crystals with distinct lattice fringes confirming the crystalline nature of the as-synthesised silver nanoparticles. The micrograph shows the presence of well separated individual lattice fringes with the measured lattice spacing (d) of 0.227 nm corresponding to the d (1 1 1) spacing for face-centered cubic (fcc) silver. The selected area electron diffraction (SAED) pattern in Fig. 2E further confirmed the crystalline nature of the particles and indicate that they are single crystals with fcc structure. The EDS spectrum (Fig. 2F) clearly confirmed the formation of silver nanoparticles without any impurity. The presence of copper comes from the copper grid used for the EDS sample preparation.

The typical XRD pattern of the as-synthesised Ag-NPs is shown in Fig. 3. Five diffraction peaks at 2θ values of 19.8°, 38.9°, 45°, 64.1°, and 76.0° were observed. The broad peak between 15° and 20° is due to the amorphous gelatin phase used as the capping agent. The four peaks at 38.9°,45°, 64.1° and 76.0° are attributed to the (1 1 1), (2 0 0), (2 0 0) and (3 1 1) crystalline planes of the face centered cubic (fcc) crystalline structure of metallic silver, respectively (JCPDS file No. 00-004-0783). The broad nature of the XRD peaks could be attributed to the nanocrystalline nature of the Ag-NPs. The surface chemistry of the as-synthesised dextrose reduced gelatin capped Ag-NPs was investigated using FT-IR spectroscopy to confirm the capping by gelatin (Fig. 3 inlet). The minor peak at 1045 cm^{-1} is attributed to the —C—O vibrations from the gelatin. Two small peaks at 1084 cm^{-1} and 1377 cm^{-1} are attributed to the —C—O stretching and O—H stretching. A small peak at 1465 cm^{-1} is due to the amide linkage vibration, i.e. —N—H stretching of the gelatin. A significant peak at 1641 cm^{-1} is due to the —C=O stretching of the —COOH group of the gluconic acid. This confirmed the reducing action of the dextrose. The broad peak at 3342 cm^{-1} is due to the —O—H stretching vibration. The slight shift in the OH and N—H bands of the gelatin-capped Ag-NPs compared to free gelatin indicated that, there is electrostatic crosslinking between the Ag-NPs and the gelatin, thus confirming the capping of the Ag-NPs by gelatin. Such interaction also enhances the interaction between gelatin molecules and ameliorates the stability of the as-synthesized gelatin capped Ag-NPs (Oluwafemi et al., 2013a,b)

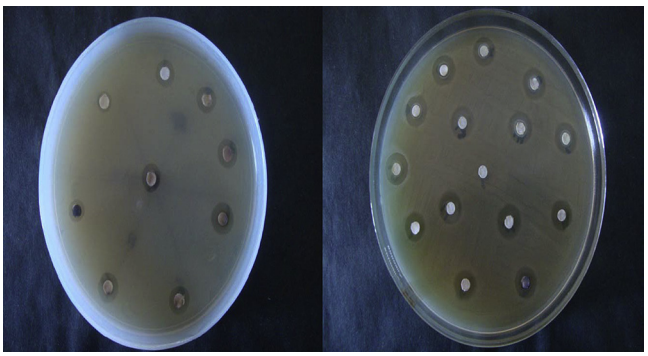

Fig. 4. Comparison of the inhibition zone test for Gram-negative bacteria (a) *E. coli* and (b) *P. aeruginosa*.

3.2. Antimicrobial study

On incubation, the plates in which disc diffusion was carried out were checked for the presence of zone of growth inhibition around the antibiotic discs and those discs loaded with nanoparticles. Fig. 4 illustrate the images of each inhibition zones. The diameter of each inhibition zones was measured and the results of the finding are shown in Table 1. The results show that, there was zone of growth inhibition around all the discs tested against the *E. coli* except for the ciprofloxacin disc. In case of *P. aeruginosa*, there was zone of inhibition around all the discs except the two antibiotic discs. The preliminary disc diffusion method showed that all the as-synthesized Ag-NPs had antibacterial activity against the two bacteria under study. At the same time both bacteria were showed to be resistant to the present drug of choice ciprofloxacin. *E. coli* was found to be sensitive to imipenem, whereas *P. aeruginosa* was resistant to the antibiotic highlighting its drug resistant nature. The MIC of the samples was evaluated using the microtube broth dilution technique and the results of the finding are shown in Table 2. The MIC of the silver nanoparticles at different reaction times was found to be between 10–12.5 μg/mL against *E. coli* and between 6–18.37 μg/mL against *P. aeruginosa*. The MBC were between 12.5–18.37 for both *E. coli* and *P. aeruginosa* respectively. The MIC of the antibiotics were also evaluated and were found to be 16 μg/mL for both *E. coli* and *P. aeruginosa* in the case of imipenem. In the case of ciprofloxacin, the MIC was found to be 10 and 20 μg/mL respectively for *E. coli* and *P. aeruginosa*. The as-synthesied Ag-NPs at different reaction times show better efficacy against the two bacteria than imipenem and silver nitrate, and a better efficacy against *P. aeruginosa* than ciproflaxin. However,

Table 1
Average diameter of inhibition zone for gelatin coated silver nanoparticles against *E. coli* and *P. aeruginosa*.

Sl. No.	Sample	Diameter of zone of inhibition (mm)	
		E. coli	*P. aeruginosa*
1	1 h	08	12,5
2	5 h	11	13
3	18 h	12	13
4	24 h	13	12
5	48 h	12	14
6	$AgNO_3$	11	13
7	Imipenem (10 mg)	15	Not appearing
8	Ciprofloxacin (5 mg)	Not appearing	Not appearing

Table 2
MIC and MBC values of the silver nanoparticles against *E. coli* and *P. aeruginosa*.

Sl. No.	Sample code	*E. coli* ATCC		*P. aeruginosa*	
		MIC (μg/ml)	MBC (μg/ml)	MIC (μg/ml)	MBC (μg/ml)
1	1 h	10	12.5	6	12.5
2	5 h	12.5	12.5	6	12.5
3	18 h	12.5	12.5	12.5	12.5
4	24 h	12.5	12.5	12.5	12.5
5	48 h	12.5	18.37	18.37	18.37
6	$AgNO_3$ (fresh)	18.37	18.37	18.37	18.37
7	Imipenem	16		16	
8	Ciprofloxacin	10		20	

the antibiotic ciproflaxin, showed a stronger antibacterial activity against *E. coli* than most of the as-synthesised Ag-NPs. Contrary to the reports that, the smaller the Ag-NPs the higher the antimicrobial activity, the results of this analysis showed that, the smaller Ag-NPs produced at higher reaction time showed lower antibacterial activity. This anomaly has been attributed to the effective passivation of the smaller Ag-NPs surface by the gelatin, thus reducing its toxicity as well as its antimicrobial activity. However, the antimicrobial activity is still stronger than silver nitrate except for Ag-NPs produced at 48 h reaction time. Furthermore, the as-synthesised Ag-NPs also have bactericidal effects resulting not only in inhibition of bacterial growth but also in killing bacteria. This irreversible inhibition of bacterial growth has been reported to be desirable to prevent bacterial colonization of silver-containing medical devices, such as catheters (Rupp et al., 2004; Samuel & Guggenbichler, 2004) where bacteria-killing activity is required. The MBC of the of the as-synthesised Ag-NPs against Gram-negative bacteria were the same as MIC for some of the samples (See Table 2) and were higher than the value obtained for silver nitrate except for 48 h sample. These results clearly show that the as-synthesised

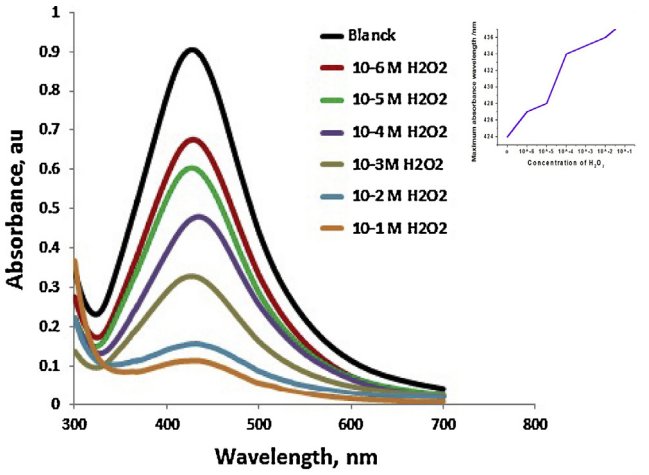

Fig. 5. Change in the LSPR peak position after the addition of H_2O_2 at different concentration. Inset: graph of H_2O_2 concentration against the SPR peak position

dextrose reduced, gelatin capped-Ag-NPs can inhibit the growth and multiplication of the tested bacteria.

3.3. Sensing property of silver nanoparticles towards H_2O_2

Fig. 5 shows the change in the maximum SPR peak position of the Ag-NPs after the addition of H_2O_2 at different concentrations. The absorbance was measured 60 s after the addition of H_2O_2 solution. A red-shift in the LSPR peak position from 426 to 438 nm was observed after the addition of H_2O_2 solution. In addition, the colour of the solution changes gradually from yellow to colourless depending on the concentration of the hydrogen peroxide. This hyperchromic shift in the LSPR peak position and the change in the colour of the solution have been attributed to the catalytic ability

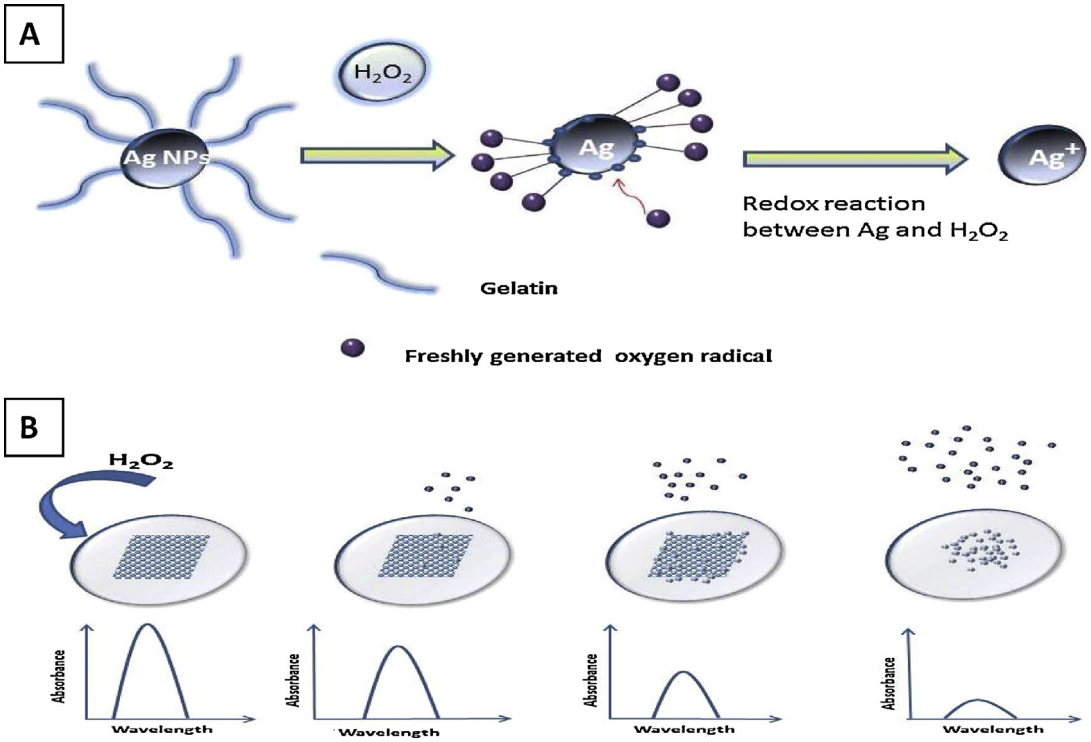

Fig. 6. Possible mechanism and schematic representation of (a) reaction between Ag-NPs and H_2O_2 and (b) decrease in the absorbance intensity with increase in concentration of H_2O_2.

of silver for the decomposition of hydrogen peroxide (Pal, Maity, & Ganguly, 1988). The reaction between the Ag-NPs and H_2O_2 caused the destruction of the gelatin coating of the Ag-NPs thus, making the aggregation of the nanoparticles inevitable and therefore increased in the particle size as evident by the red-shifting of the LSPR peak position (Fig. 5 inset). A schematic representation of the possible mechanism is given in Fig. 6(a). When the concentration of the H_2O_2 solution added to the Ag-NPs increased, a decrease in the λ_{max} intensity was observed. The observed decrease in the absorbance intensity implies decrease in the Ag-NPs concentration (Fig. 6B). The decrease in the absorbance is proportional to the concentration of the H_2O_2 solution. The higher the peroxide concentration, the stronger the decrease in the Ag-NPs concentration and hence, lowering of the Ag-NPs LSPR peak intensity. A schematic representation of the catalytic action of Ag-NPs in the presence of H_2O_2 is given in Fig. 6(b). The nanoparticles used here are protected by a gelatin layer. The catalytic action between silver and hydrogen peroxide occurs through the protection layer of gelatin around the Ag-NPs. The introduction of ROS species like H_2O_2 in the solution, forms reactive radical species and initiates the degradation of the gelatin protected Ag-NPs. This results in the oxidation of Ag to Ag^+ ions and thereby decreases in the LSPR absorbance.

4. Conclusion

We have successfully synthesized water soluble, monodispersed and highly stable silver nanoparticles via a completely green and facile method. Gelatin, dextrose and water were used as the capping agent, reducing agent and solvent respectively. The as-synthesized Ag-NPs were small, spherical, nearly monodispersed and highly crystalline with face centered cubic crystal structure. The as-synthesized Ag-NPs show high antibacterial activity against Gram negative bacteria such as *E. coli* and *P. aregunosa* and can inhibit the growth and multiplication of the tested bacteria. The degradation of silver nanoparticles induced by the catalytic decomposition of hydrogen peroxide causes a considerable change in the LSPR absorbance depending on the H_2O_2 concentration. This sensor reaction has a very good sensitivity and a linear response over wide H_2O_2 concentration range of 10^{-1}–10^{-6} M H_2O_2.

Acknowledgements

The authors thank the Department of Science and Technology (DST Nano mission (SR/NM/NS-54/2009)), National research foundation (NRF) South Africa, under the Nanoflagship Programme (Grant no: (68706) and CV Raman Fellowship programme for financial support. The financial support from UGC-Government of India through SAP and DST -Government of India through FIST and PURSE programme are also gratefully acknowledged. This is the part of the work that OS Oluwafemi did whilst a visiting fellow at Centre for Nanoscience and Nanotechnology, Mahatma Gandhi University, Kerala, India, under CV Raman Fellowship for African researchers. He thanks the DST (India) for the Fellowship and Prof. Sabu Thomas and his research group for being gracious hosts.

References

Batabyal, S. K., Basu, C., Das, A. R., & Sanyal, G. S. (2007). Green chemical synthesis of silver nanowires and microfibers using starch. *Journal of Biobased Materials and Bioenergy*, *1*, 143–147.

Bozanic, D. K., Trandafilovic, L. V., Luyt, A., & Djokovic, S. V. (2010). 'Green' synthesis and optical properties of silver–chitosan complexes and nanocomposites. *Reactive and Functional Polymers*, *70*, 869–873.

Chreigton, J. A., Blatchford, C. G., & Albrecht, M. G. (1979). Plasma resonance enhancement of Raman scattering by pyridine adsorbed on silver or gold sol particles of size comparable to the excitation wavelength. *Journal of the Chemical Society Faraday Transactions 2*, *75*, 790–798.

Darroudi, M., Ahmad, M. B., Abdullah, A. H., & Ibrahim, N. A. (2011). Green synthesis and characterization of gelatin-based and sugar-reduced silver nanoparticles. *International Journal of Nanomedicine*, *6*, 569–574.

Darroudi, M., Ahmad, M. B., Zamiri, R., Zak, A. K., Abdullah, A. H., & Ibrahim, N. A. (2011). Time-dependent effect in green synthesis of silver nanoparticles. *International Journal of Nanomedicine*, *6*, 677–681.

Eid, K. A., & Assay, H. M. (2012). Controlled synthesis and characterization of hollow flower-like silver nanostructures. *International Journal of Nanomedicine*, *7*, 1543–1550.

Endo, T., Yanagida, Y., & Hatsuzawa, T. (2008). Quantitative determination of hydrogen peroxide using polymer coated Ag nanoparticles. *Measurement*, *41*, 1045–1053.

Filippo, E., Serra, A., & Manno, D. (2009). Poly(vinyl alcohol) capped silver nanoparticles as localized surface plasmon resonance-based hydrogen peroxide sensor. *Sensors and Actuators B*, *138*, 625–630.

Filippo, E., Serra, A., Buccolieri, A., & Manno, D. (2010). Green synthesis of silver nanoparticles with sucrose and maltose: Morphological and structural characterization. *Journal of Non-Crystalline Solids*, *356*, 344–350.

Hermanson, K. D., Lumsdon, S. O., Williams, J., Kaler, P., & Velev, E. W. O. D. (2001). Dielectrophoretic assembly of electrically functional microwires from nanoparticle suspensions. *Science*, *294*, 1082–1086.

Jennifer, A. D., Bettye, L. S., & Maddux James, E. H. (2007). Towards greener nanosynthesis. *Chemical Reviews*, *107*, 2228–2269.

Kim, J. S., Eunye, K., Kim, J. H., Park, S. J., & Park, Y. H. (2007). Antimicrobial effects of silver nanoparticles. *Nanomedicine: Nanotechnology, Biology and Medicine*, *3*, 95–101.

Lee, P. C., & Meisel, D. (1982). Adsorption and surface-enhanced Raman of dyes on silver and gold sols. *The Journal of Physical Chemistry*, *86*, 3391–3396.

Oluwafemi, O. S., Lucwabaa, Y., Guraa, A., Masabeyaa, M., Ncapayia, V., Olujimia, O. O., Songca, S. P., et al. (2013a). A facile completely 'green' size tunable synthesis of maltose-reduced silver nanoparticles without the use of any accelerator. *Colloids and Surfaces B: Biointerfaces*, *102*, 718–723.

Oluwafemi, O. S., Ncapayi, V., Scriba, M., & Songca, S. P. (2013b). Green controlled synthesis of monodispersed, stable and smaller sized starch-capped silver nanoparticles. *Materials Letters*, *106*, 332–336.

Pal, T., Maity, D. S., & Ganguly, A. (1988). Silver-gelatin method for determination of inorganic peroxides in alkaline solution. *Talanta*, *35*, 658–660.

Panacek, A., Kvitek, L., Prucek, R., Kolar, M., Vecerova, R., Pizurova, N., et al. (2006). Silver colloid nanoparticles: synthesis, characterization, and their antibacterial activity. *Journal of Physical Chemistry B*, *110*, 16248–16253.

Raveendran, P., Fu, J., & Wallen, S. L. (2003). Completely green synthesis and stabilization of metal nanoparticles. *Journal of American Chemical Society*, *125*, 13940–13941.

Raveendran, P., Fu, J., & Wallen, S. L. (2006). A simple and "green" method for the synthesis of Au Ag, and Au–Ag alloy nanoparticles. *Green Chemistry*, *8*, 34–38.

Rupp, M. E., Fitzgerald, T., Marion, N., Helget, V., Puumala, S., Anderson, J. R., et al. (2004). Effect of silver-coated urinary catheters: efficacy, cost-effectiveness, and antimicrobial resistance. *American Journal Infection Control*, *32*, 445–450.

Samuel, U., & Guggenbichler, J. P. (2004). Prevention of catheter-related infections: The potential of a new nano-silver impregnated catheter. *International Journal of Antimicrobial Agents*, *23*, S75–S78.

Stevanovic, M., Kovacevic, B., Petkovic, J., Filipic, M., & Uskokovic, D. (2011). Effect of poly-α,(L-glutamic acid as a capping agent on morphology and oxidative stress-dependent toxicity of silver nanoparticles. *International Journal of Nanomedicine*, *6*, 2837–2847.

Zhenhua, Z., Wang, S., Zhou, W., Wang, G., Jiang, L., Li, W., et al. (2003). Novel synthesis of highly active Pt/C cathode electrocatalyst for direct methanol fuel cell. *Chemical Communication*, 394–395.